Electronic Supplementary Material (ESI) for Nanoscale.

Supplementary Information

Thermally Reversible Pattern Formation in Arrays of Molecular Rotors

Marcello DeLuca[1], Wolfgang G. Pfeifer[2,3], Benjamin Randoing[4], Chao-Min Huang[1], Michael G. Poirier[3], Carlos E. Castro[2], Gaurav Arya[1,*]

[1]Department of Mechanical Engineering and Materials Science, Duke University

[2]Department of Mechanical and Aerospace Engineering, The Ohio State University

[3]Department of Physics, The Ohio State University

[4]Department of Biomedical Engineering, Duke University

*Email: gaurav.arya@duke.edu, Tel: +1-919-660-5435, Fax: +1-919-660-8963

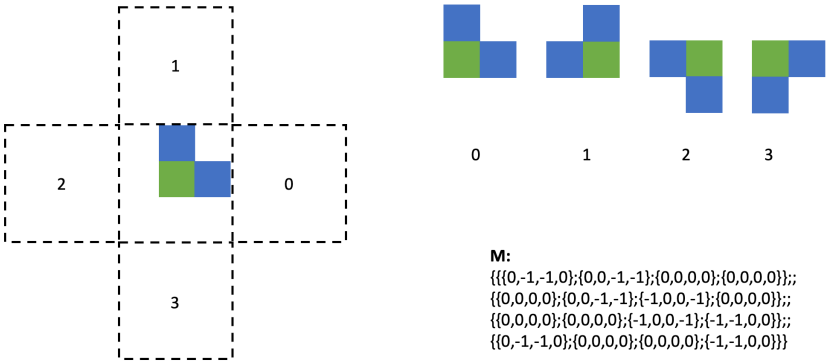

Figure S1: Diagram of system states and neighbor indices for L-shaped rotor.

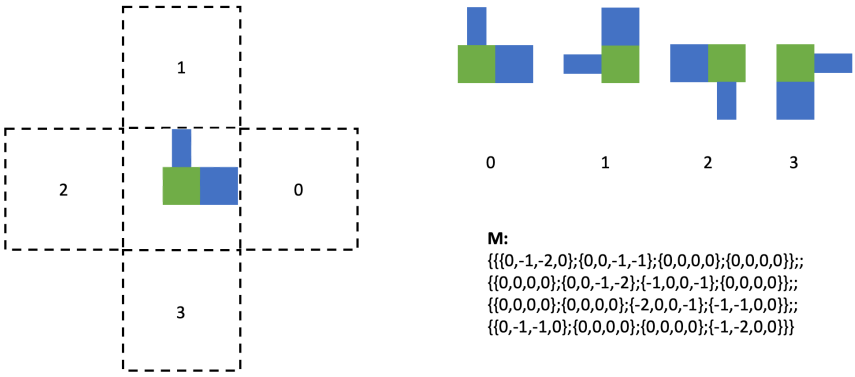

Figure S2: Diagram of system states and neighbor indices for chiral rotor.

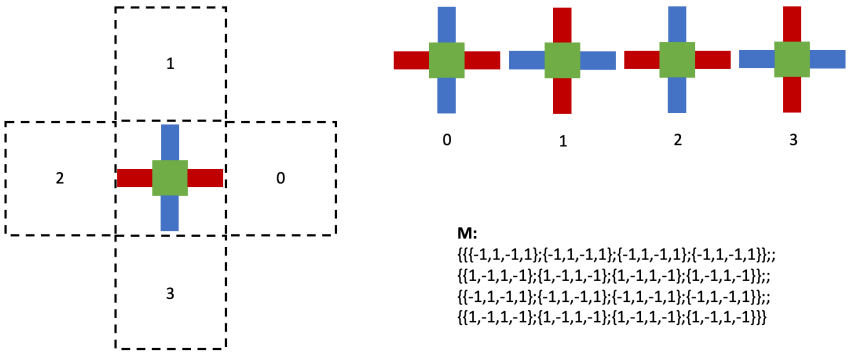

Figure S3: Diagram of system states and neighbor indices for 2D Ising-like rotor.

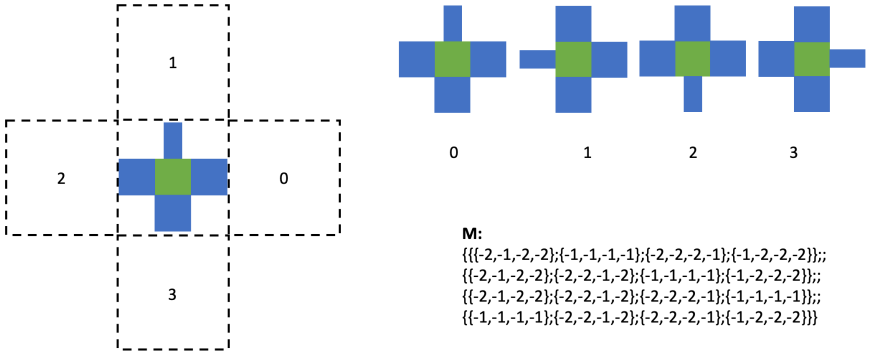

Figure S4: Diagram of system states and neighbor indices for 2-2-2-1 rotor.

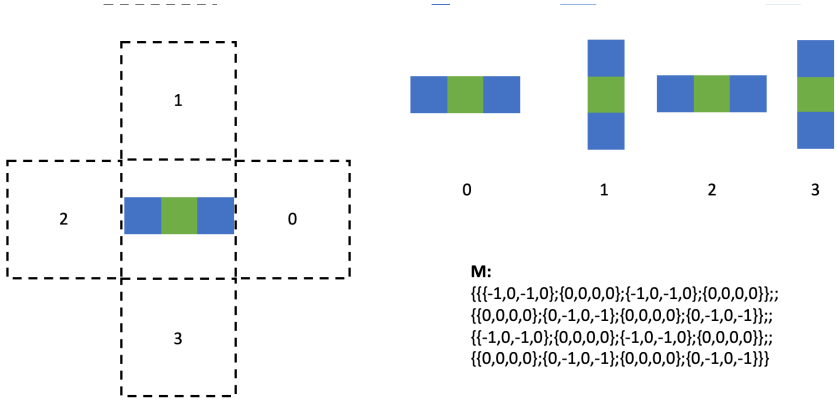

Figure S5: Diagram of system states and neighbor indices for quasi-1D Ising rotor.

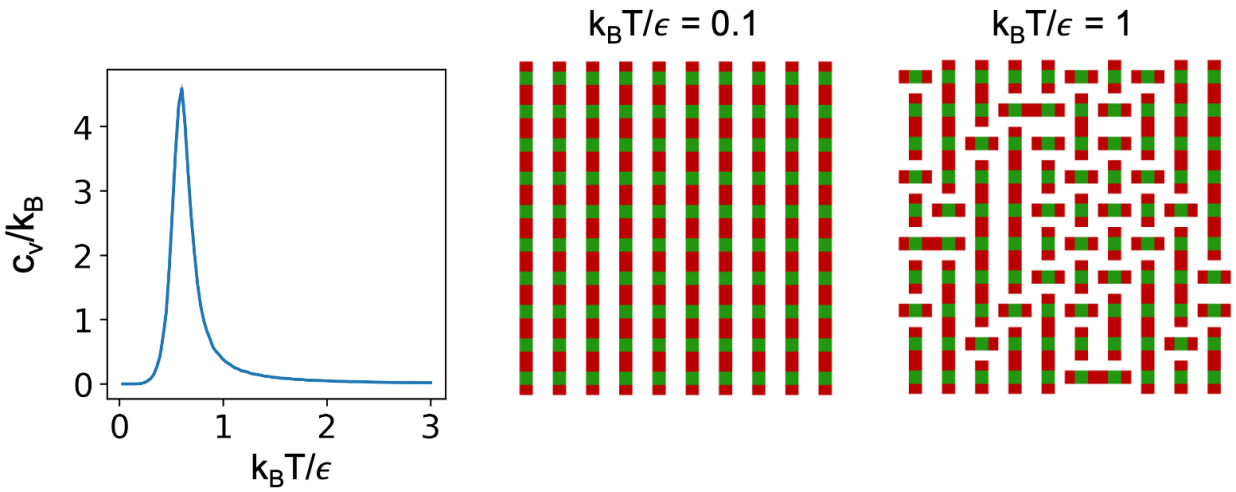

Figure S6: Specific heat curve for 10x10 quasi-1D Ising system.

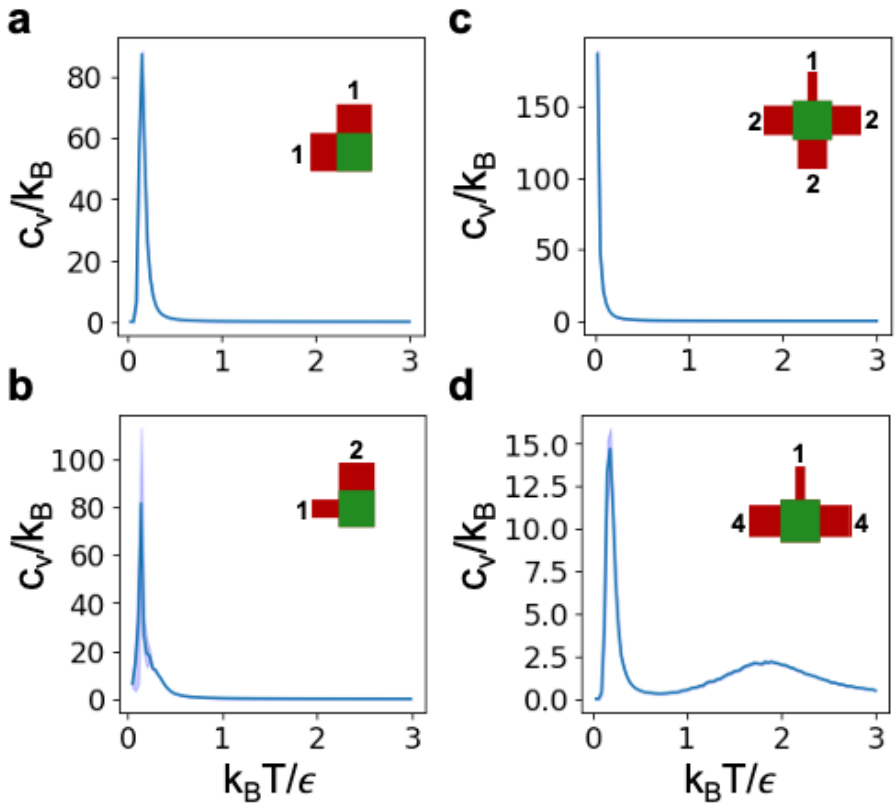

Figure S7: Specific heat curves for four designs with no periodic boundary conditions: (a) L-shaped rotor, (b) Chiral rotor, (c) 2-2-2-1 rotor, and (d) 4-1-4 rotor.

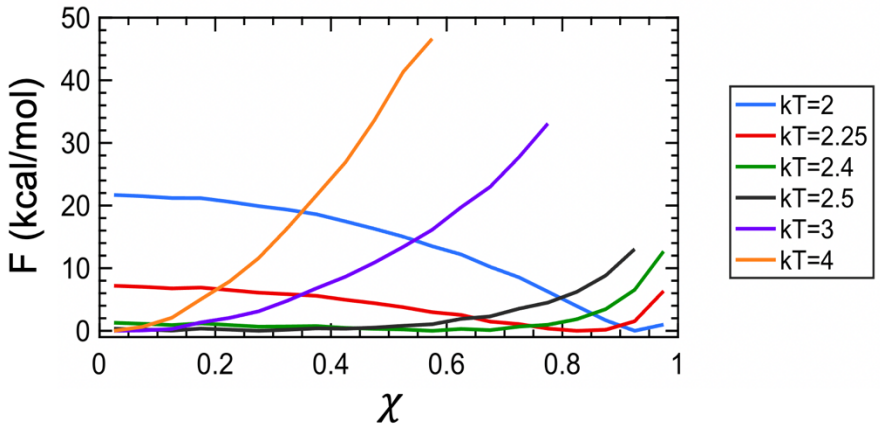

Figure S8: Free energy computed as a function of χ at various temperatures for the 2D Ising lattice using umbrella sampling Monte Carlo simulations.

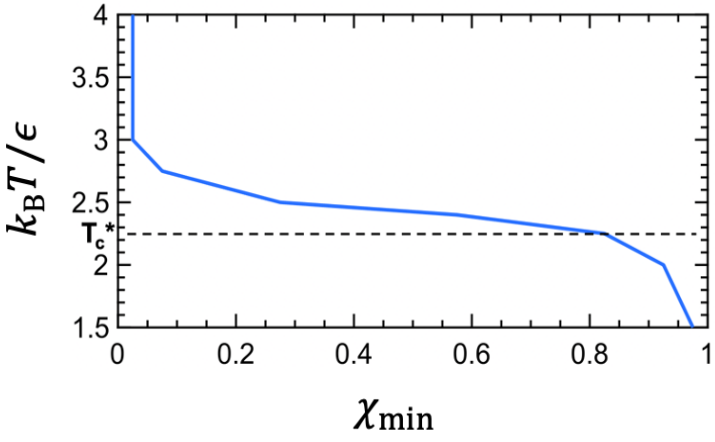

Figure S9: Free energy-minimizing value of χ as a function of temperature, demonstrating a transition in the Ising lattice. χ acts analogous to the more commonly used order parameter, average magnetization.

Table S1: Thermal annealing protocol to fold DON rotor devices.

T [°C]	**t [min/°C]**
65	15
64-61	5
60	8
59-58	12
57	15
56	25
55	36
54	45
53-49	60
48-45	45
44	40
43-42	36
41-38	24
37-20	10

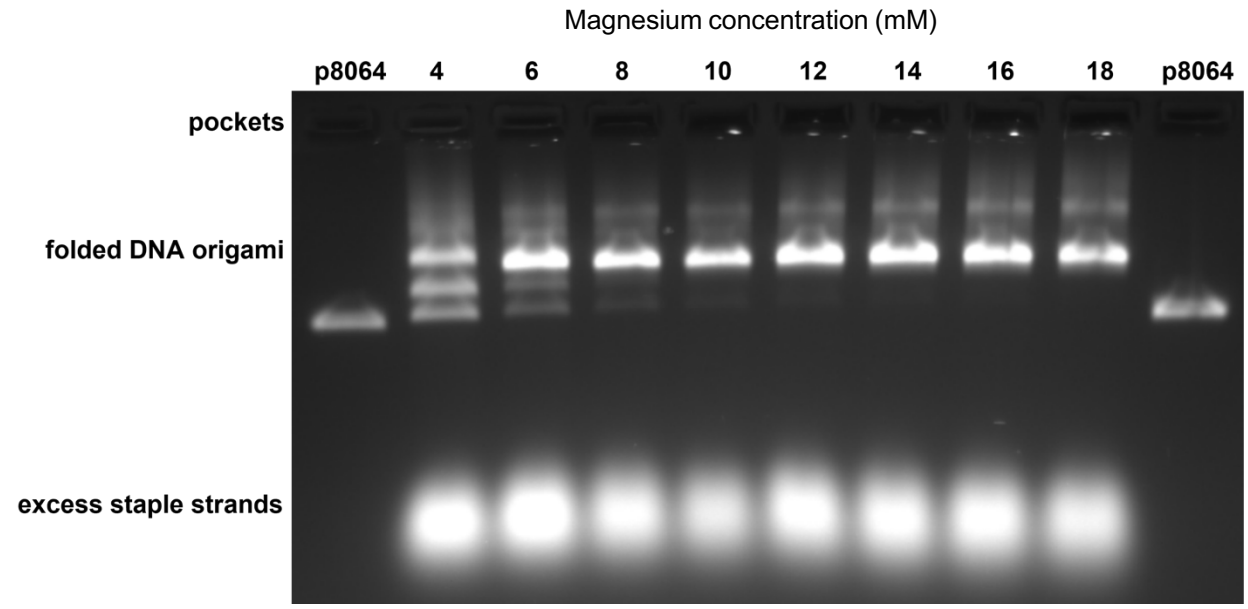

Figure S10: Agarose gel electrophoresis of a Magnesium screening, indicating the conditions to properly fold the DON rotor device.

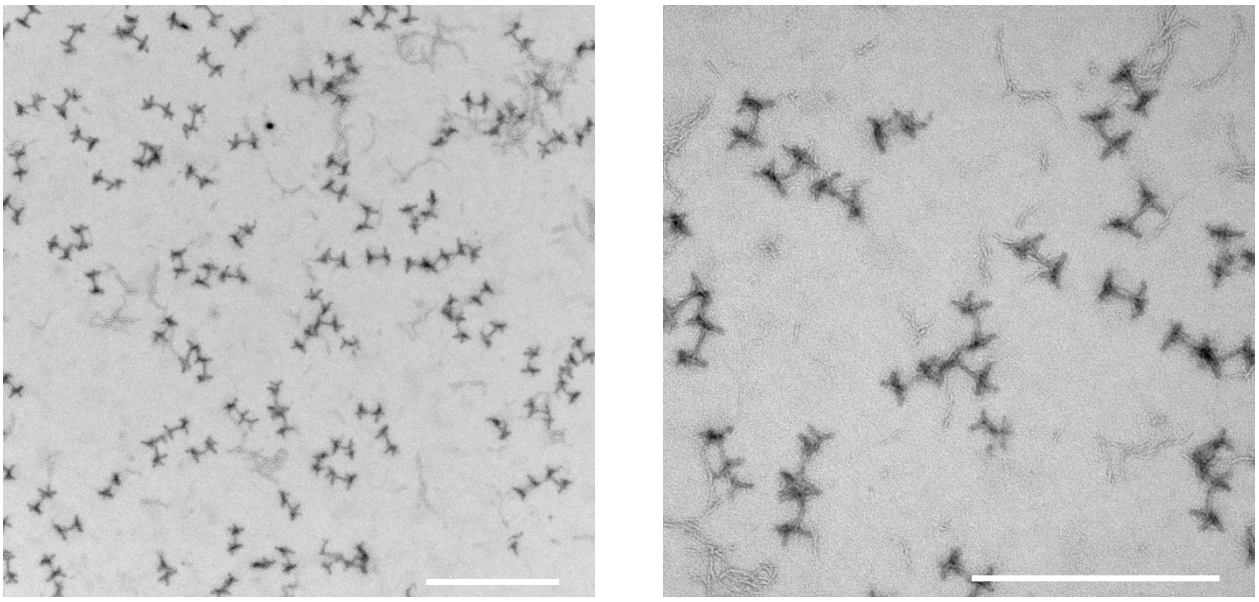

Figure S11: TEM micrographs of monomeric DON rotor devices (without overhangs). Scale bar: 500 nm.

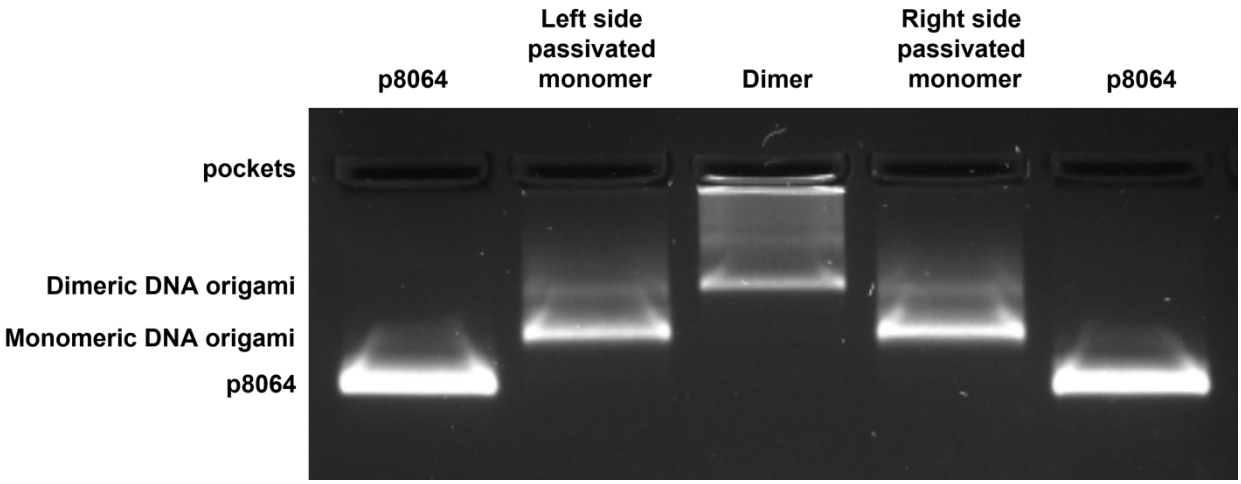

Figure S12: Agarose gel electrophoresis of monomers and dimers of the DON. Dimer bands were then excised and extracted using a BioRad Freeze ‘ N Squeeze kit.

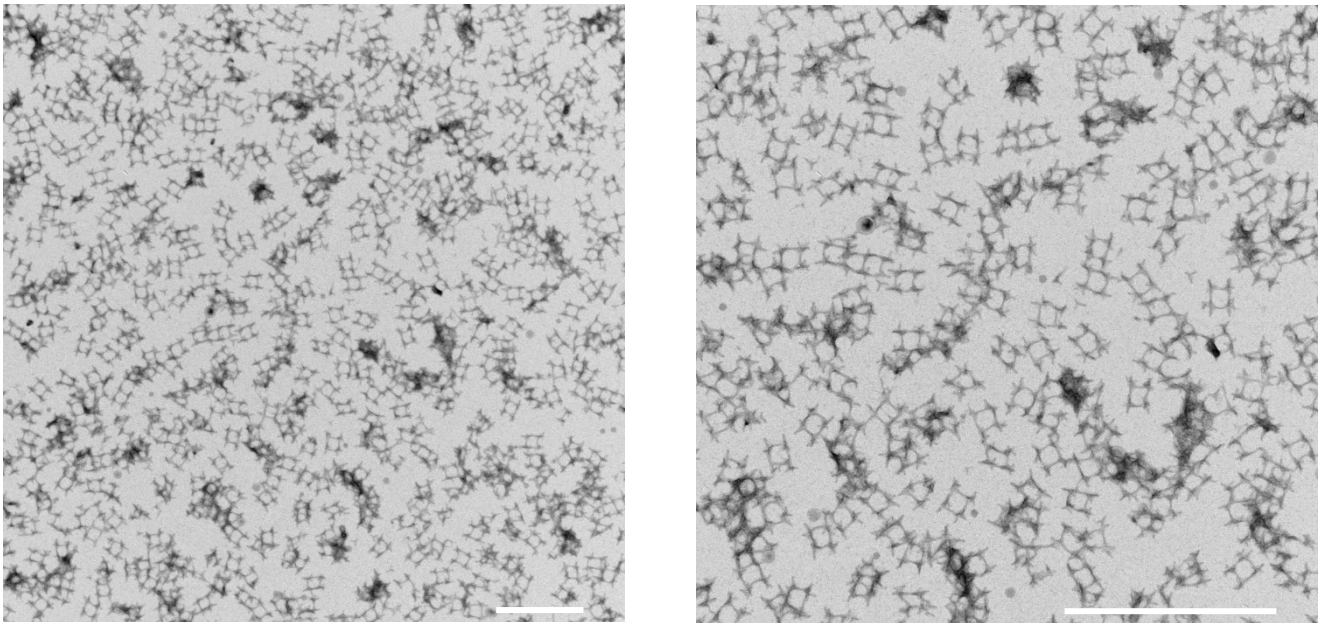

Figure S13: Exemplary TEM micrographs of dimeric DON rotor devices. Scale bar: 500 nm.

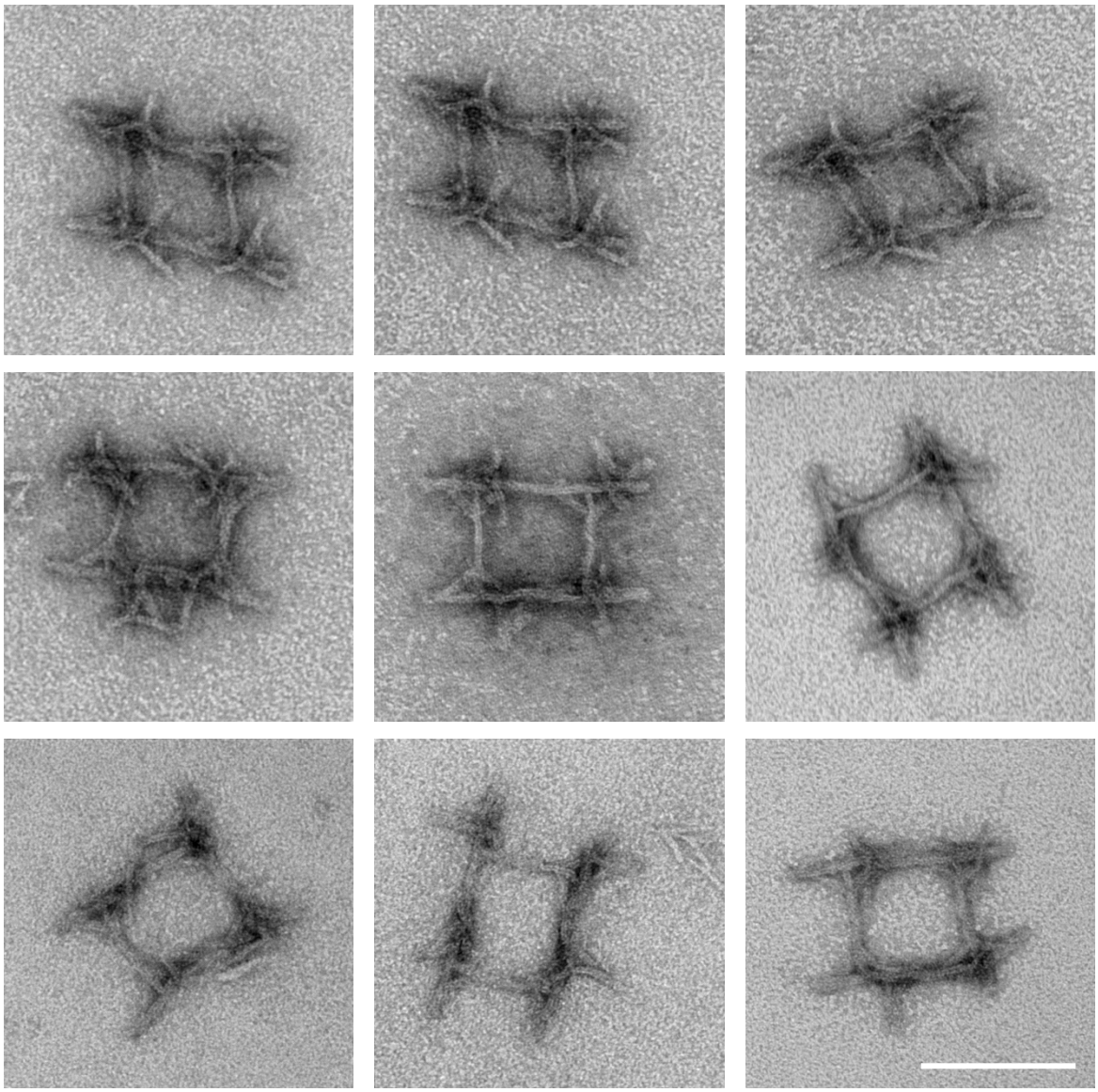

Fig. S14: Exemplary TEM images of rotors on 2x2 arrays, showing no alignment. Scale bar: 100 nm.

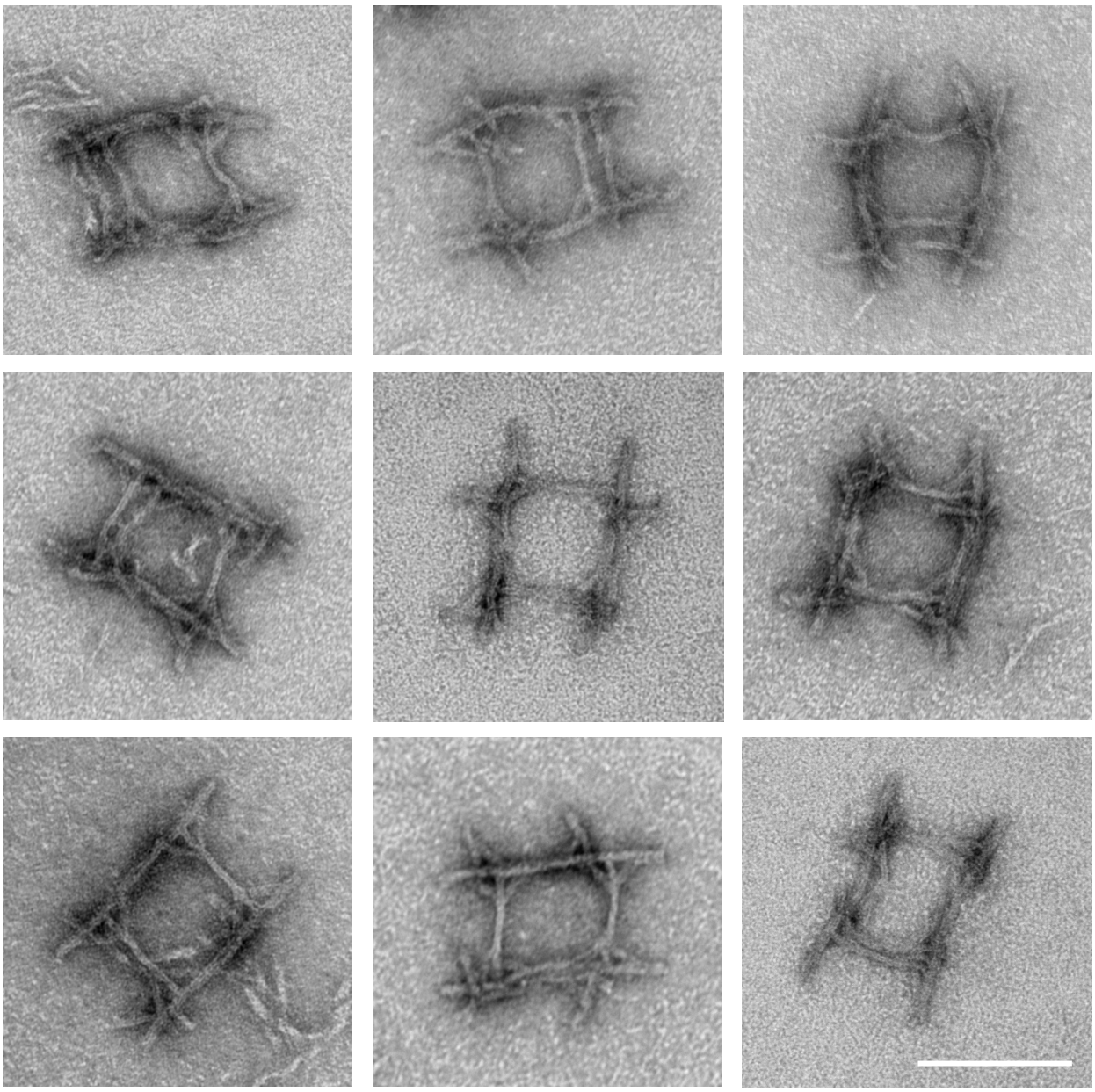

Fig. S15: Exemplary TEM images of rotors on 2x2 arrays, showing partial alignment. Scale bar: 100 nm.

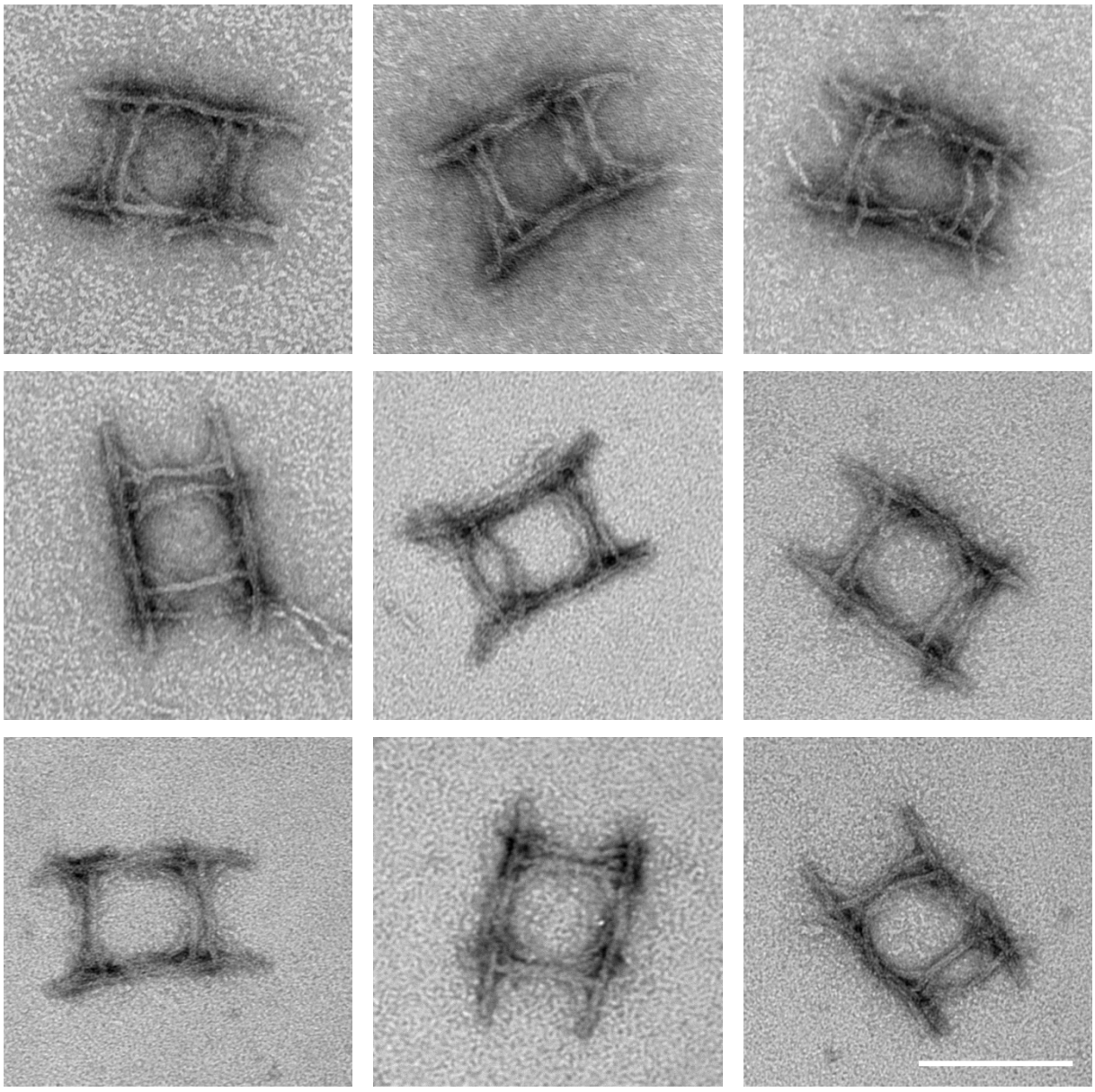

Fig. S16: Exemplary TEM images of rotors on 2x2 arrays, showing full alignment. Scale bar: 100 nm.

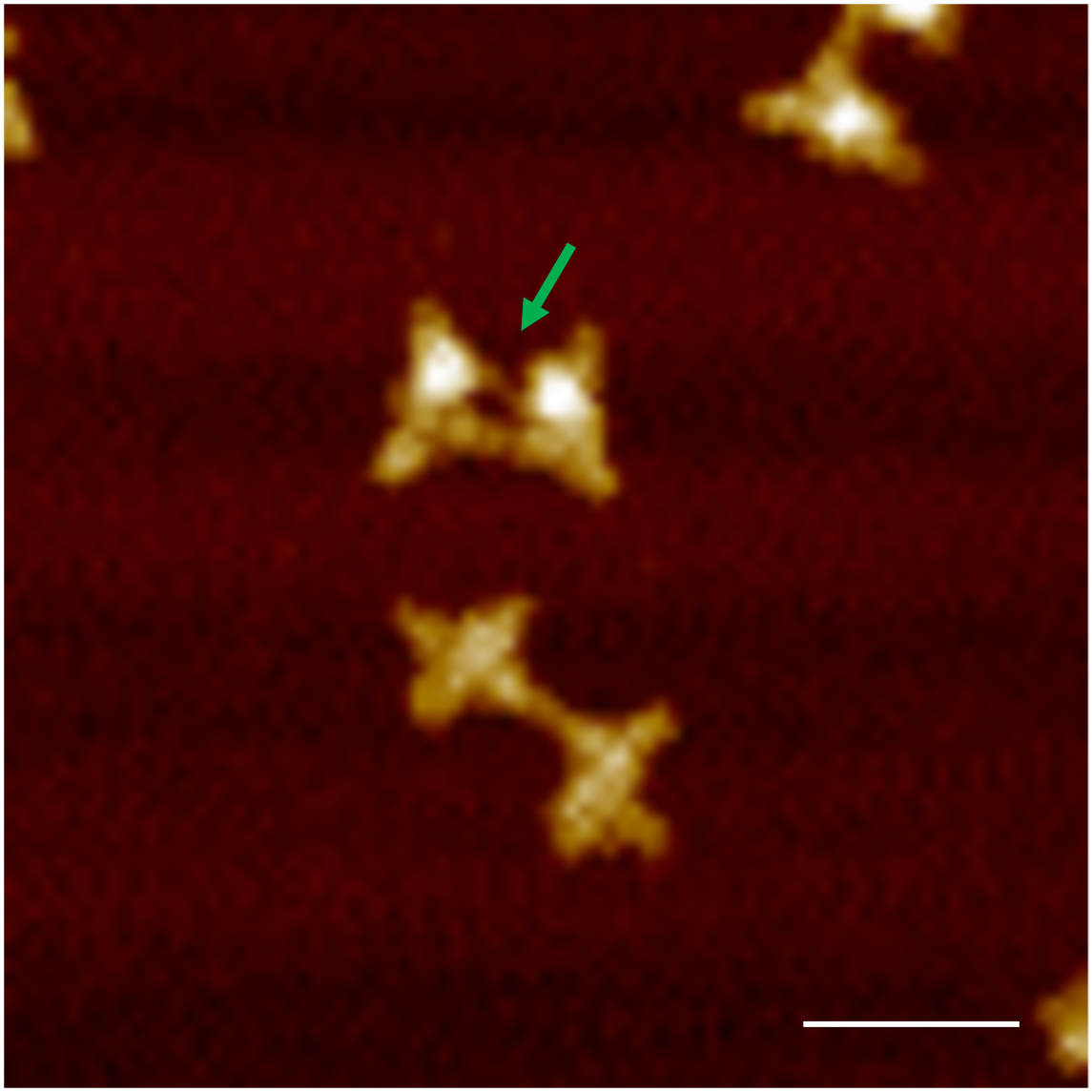

Fig. S17: AFM image showing the formed dsDNA connection between the complementary overhangs (green arrow). Scale bar: 100 nm.

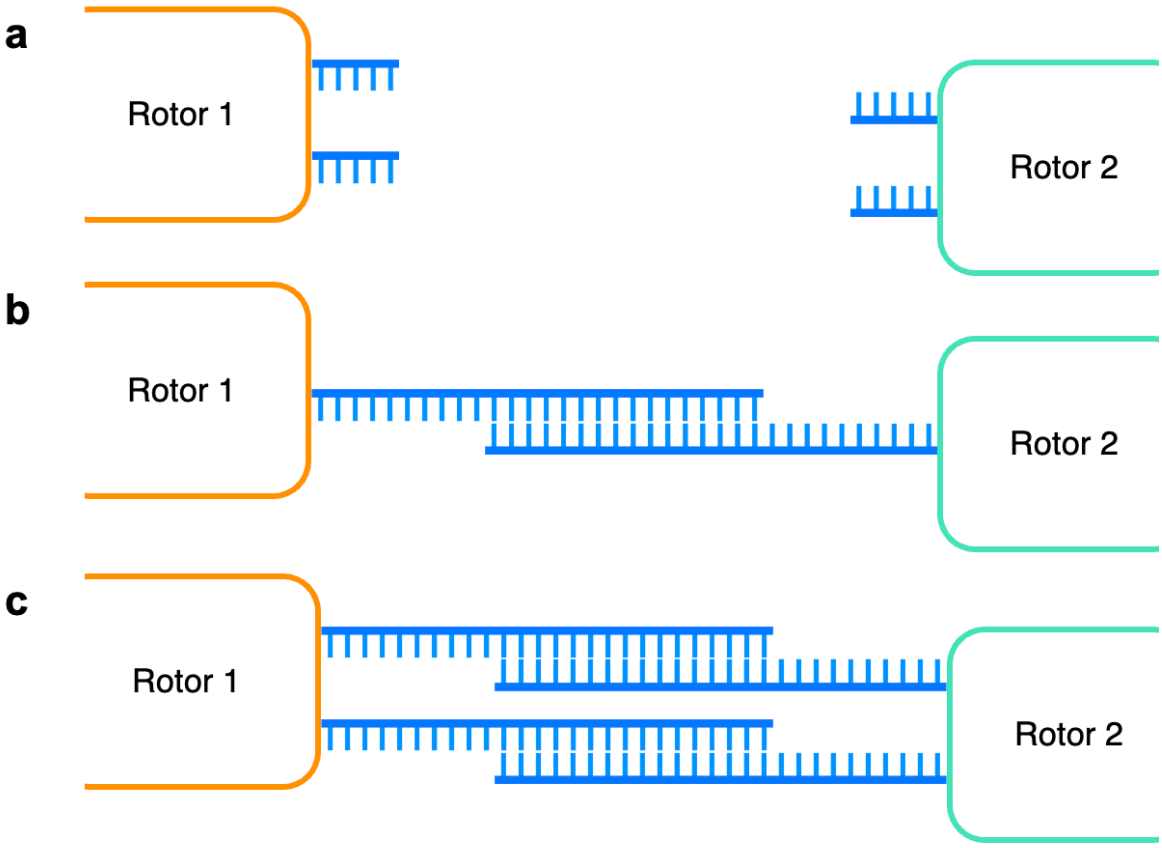

Fig. S18: Different number of interacting overhangs for rotor-rotor interactions. (a) No complementary overhangs are attached to the rotors. (b) one set of complementary overhangs is attached to the rotors. (c) two sets of complementary overhangs is attached to the rotors.

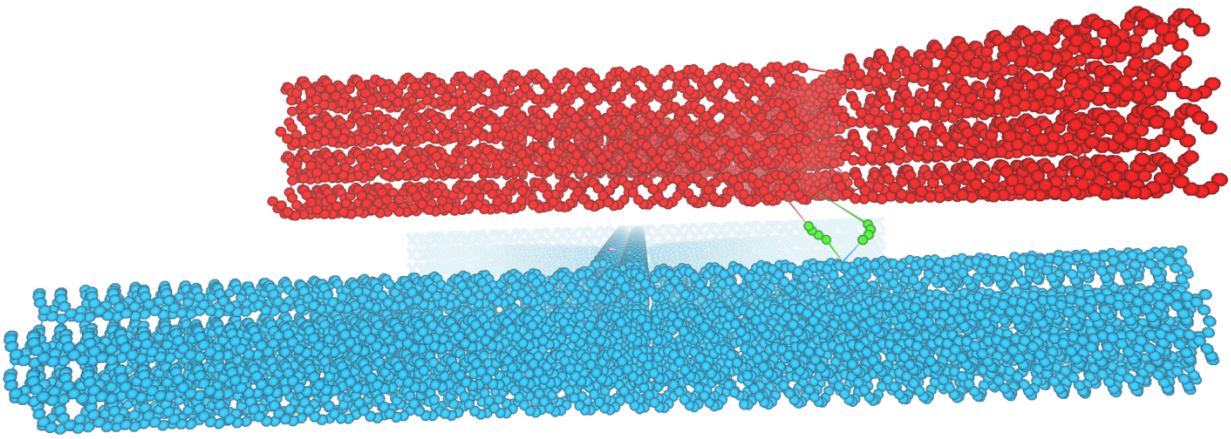

Fig. S19: Rotor–base connection with two stretches of 4 bases of unpaired scaffold (green). Backbone bonds are not relaxed to create a larger gap between base and rotor. This schematic contains only one rotor to reduce distractions in the background. The base is shown in blue and the rotor is shown in red, but both components are assembled in a single step.

Supplementary Note 1:
The addition of overhangs to allow rotor-rotor interactions is performed as a final step in the assembly of the 2x2 arrays to prevent undesired aggregation. We initially tested the inclusion of these overhangs during the initial thermal assembly, but observed multiple bands in agarose gel electrophoresis, indicating aggregation. We assume that lower concentrations of DON at the final stage of the assembly help to reduce aggregation. Additionally, reducing the time between addition of the overhangs and imaging might help to mitigate these undesired interactions. Figure **S20** shows an agarose gel comparing DON with and without overhangs after folding.

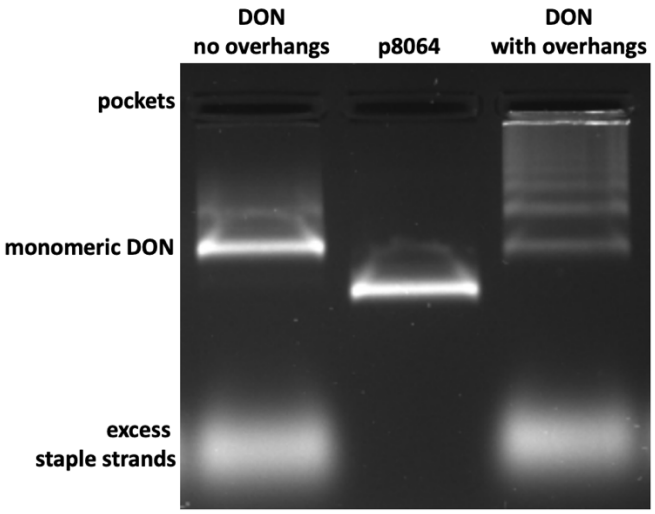

Figure S20: Comparison of DON folded in the absence (left lane) or presence (right lane) of rotor-rotor interaction overhangs.

Supplementary Note 2:

Design:

The full design of the two-rotor DON will be available on nanobase.org.

Sequences:

Overhang sequences to allow rotor-rotor interaction. The stretch of these oligonucleotides which binds to the scaffold is not shown here. Unpaired bases used as spacer are shown italicized.

Sequence 1: TCTGGTTAACGTGTCT*ttttttttt*

Sequence 2: AGACACGTTAACCAGA*ttttttttt*

All oligonucleotide sequences can be found in an Excel spreadsheet in the **data package.**